CLIMATE SYSTEM MODELING IN THE FRAMEWORK OF THE TOLERABLE WINDOWS APPROACH: THE ICLIPS CLIMATE MODEL

THOMAS BRUCKNER [1], GEORG HOOSS [2], HANS-MARTIN FÜSSEL [3] and KLAUS HASSELMANN [2]

[1] *Institute for Energy Engineering, Technical University of Berlin, Marchstr. 18, D-10587 Berlin, Germany*
E-mail: bruckner@iet.tu-berlin.de
[2] *Max Planck Institute for Meteorology, Bundesstraße 55, D-20146 Hamburg, Germany*
[3] *Potsdam Institute for Climate Impact Research, Telegrafenberg, D-14473 Potsdam, Germany*

Abstract. The computational burden associated with applications of the Tolerable Windows Approach (TWA) considerably exceeds that of traditional integrated assessments of global climate change. As part of the ICLIPS (Integrated Assessment of Climate Protection Strategies) project, a computationally efficient climate model has been developed that can be included in integrated assessment models of any kind. The ICLIPS climate model (ICM) is implemented in GAMS. It is driven by anthropogenic emissions of CO_2, CH_4, N_2O, halocarbons, SF_6, and SO_2. The output includes transient patterns of near-surface air temperature, total column-integrated cloud cover fraction, precipitation, humidity, and global mean sea-level rise. The carbon cycle module explicitly treats the nonlinear sea water carbon chemistry and the nonlinear CO_2 fertilized biosphere uptake. Patterns of the impact-relevant climate variables are derived form empirical orthogonal function (EOF) analysis and scaled by the principal component of temperature change. The evolution of the latter is derived from a box-model-type differential analogue to its impulse response function convolution integral. We present a description of the ICM components and some results to demonstrate the model's applicability in the TWA setting.

1. Introduction

The main objectives of the United Nations Framework Convention on Climate Change (UNFCCC) provide a three-fold challenge to integrated assessments of the global climate change issue. First, such assessments should facilitate the identification of climate thresholds that should not be transgressed, even in the long term. Second, it is necessary to investigate the inertia of the socioeconomic system, limiting its capability to rapidly reduce emissions. Third, the short-term implications of taking into account both aspects simultaneously need to be determined.

The Tolerable Windows Approach (TWA), proposed by the German Advisory Council on Global Change (WBGU) in 1995 (WBGU, 1995, 1996; Petschel-Held and Schellnhuber, 1997; Toth et al., 1997; Petschel-Held et al., 1999), is a novel framework for addressing these issues. The objective of the TWA is to derive 'corridors' of future greenhouse-gas emissions that satisfy normative, user-defined constraints (guardrails) regarding tolerable climate change impacts and acceptable

Climatic Change **56:** 119–137, 2003.

mitigation costs. Corridors associated with pertinent control or state variables (for instance, the emissions corridors presented in detail in Toth et al., 2003a), as well as reachable state domains (like the reachable climate domains discussed in this paper) of the coupled anthroposphere-climate system are considered to be the most important results that can be derived by applying the TWA. As it is shown elsewhere (Bruckner et al., 2003), the boundaries of these corridors (and domains) can be determined by successively solving numerous independent dynamic optimization problems subject to user-defined intertemporal constraints. As the resulting computational burden is large, integrated assessment models allowing for a real application of the TWA, like the ICLIPS model (Toth et al., 2003b), must include a computationally efficient reduced-form, substitute climate model that approximates selected results obtained by sophisticated spatially resolved ocean-atmosphere-climate-chemistry models with reasonable accuracy.

The ICLIPS Climate Model (ICM) developed in the ICLIPS (Integrated assessment of CLIimate Protection Strategies) project fulfills these requirements. It is specifically designed for integration into intertemporal optimization schemes, but the applicability of the model is not restricted to integrated assessment models based on the TWA framework. As the computational burden associated with traditional computer-based cost-benefit analyses (CBA) and cost-effectiveness analyses (CEA) is small compared to TWA applications, the ICM is suitable for inclusion in CBA and CEA models as well.

The ICM consists of several modules designed to simulate (1) the atmospheric retention and metabolism of carbon dioxide and the most important other greenhouse gases, (2) their time-dependent contributions to radiative forcing, and (3) the resulting space-time-dependent anthropogenic climate change signal in several impact-relevant variables: near-surface air temperature, total column-integrated cloud cover fraction, precipitation, humidity, and sea-level rise. The modules combined to form the ICM are adaptations of peer-reviewed models that have also been used separately for a variety of other integrated assessment studies (Harvey et al., 1997; Meyer et al., 1999; Joos et al., 2001; Hooss et al., 2001). The module representing the carbon cycle and the climate change module are adapted versions of the NICCS (Nonlinear Impulse response representation of the coupled Carbon cycle – Climate System) model (Hooss, 2001), designed and developed in Fortran 77 for the ICLIPS project at the Max-Planck Institute for Meteorology, Hamburg. Atmospheric retention and metabolism of non-CO_2 greenhouse gases and aerosols, radiative forcing and sea level rise contribution from melting land ice are described according to the models underpinning the Second Assessment Report of the Intergovernmental Panel on Climate Change (IPCC) (Harvey et al., 1997). Transient spatial patterns of the impact-relevant climate variables are calculated by applying the scaled scenario approach as described by Füssel et al. (2003). For compatibility with the socioeconomic components (Leimbach and Toth, 2003) of the ICLIPS integrated assessment model, all modules of the ICM had to be reimplemented in GAMS (General Algebraic Modeling System; Brooke et al., 1992),

a programming environment frequently used by economists to solve optimization problems of various kinds.

In order to contribute to the goal of this special issue, namely to provide a comprehensive overview of the entire ICLIPS integrated framework, this paper briefly reviews all modules including the specific adaptation measures that were necessary for the GAMS implementation. In addition, selected results are presented to demonstrate the model's applicability in the TWA setting. As the results of the fully coupled ICLIPS model are discussed elsewhere (Toth et al., 2003a), we focus on results obtained by using the ICM in a stand-alone mode.

2. Model Components and Methodological Aspects

2.1. CARBON CYCLE MODELING

Following the approach first applied for integrated assessment by Harvey (1989), the module describing the uptake of anthropogenic CO_2 by the world ocean is based upon the impulse response characteristics (cf. Siegenthaler and Oeschger, 1978; Maier-Reimer and Hasselmann, 1987; Hasselmann et al., 1993; Joos et al., 1996) of a 3-dimensional gridded ocean circulation carbon transport model. The current implementation of ICM uses the impulse response function (IRF) representation of the HAmburg Model of the Ocean Carbon Cycle (HAMOCC) (Maier-Reimer, 1993).

An impulse-response function model can be used as an exact substitute for its parent 3-dimensional model as long as only the linearized response to small perturbations is required. In the case of the carbon-cycle-climate system, this linear range extends to roughly twice the preindustrial CO_2 concentration or, correspondingly, a global warming below 2.5 °C. As long as climate change does not alter the oceanic circulation significantly, the accuracy of the linear approximation is limited only by the nonlinear uptake of CO_2 through the ocean surface. At higher concentrations, additional carbon becomes less soluble, so that a smaller fraction of the additional carbon is transported in the large deep-ocean reservoir by thermohaline overturning (Maier-Reimer and Hasselmann, 1987; Joos et al., 1996).

To include the nonlinear CO_2 chemistry, the IRF model had to be translated from its standard convolution integral form into an equivalent box-model-type differential analogue (Hooss, 2001) in the form of a cascade of a few oceanic carbon-reservoir layers (Figure 1). This box model is then calibrated in the linear limit of a small CO_2 impulse, to reproduce the 3d carbon cycle model's IRF through appropriate choice of layer thicknesses and diffusion coefficients. The layers are coupled by carbon fluxes $q_j(t)$ which, in turn, are driven by differences in the layer concentrations. The uppermost layer of the analogue can be physically interpreted as representing the composite atmosphere-plus-mixed-layer system, which can be regarded as well equilibrated during the model time step of 5 years. The anthropogenic carbon $c_1(t) = c_a(t) + c_s(t)$ in the *composite* layer is partitioned into

its atmospheric and mixed-layer subsystems (measured by carbon content $c_a(t)$ and $c_s(t)$, respectively) such that chemical equilibrium is reached between CO_2, its dissociation products, borate, and water. While the carbon flux q_2 (Figure 1) from the composite layer into the second oceanic layer is still linear at large partial pressures of CO_2, the mixed layer carbon content anomaly $c_s(t)$ becomes a nonlinear function of the composite-layer carbon anomaly $c_1(t)$. The function $c_s(c_1)$ (see the diagram embedded in Figure 1) captures all the information required to model nonlinear ocean carbon chemistry as part of a reduced-form model (Hooss, 2001). Although this function (and its companion $c_a(c_1)$) cannot be expressed in closed form, it can be calculated numerically by computing the chemical equilibrium associated with the dissolution and dissociation of CO_2 in sea water (Maier-Reimer and Hasselmann, 1987).

The ocean carbon cycle model described so far has been coupled to an adapted version of the impulse-response representation (Joos et al., 1996) of the terrestrial component of the Bern carbon cycle model (Siegenthaler and Oeschger, 1987; Siegenthaler and Joos, 1992; Kicklighter et al., 1999). In the Bern model, global terrestrial net primary production (NPP) is assumed to be proportional to the logarithm of the atmospheric CO_2 concentration. It should be emphasized that the carbon cycle model constructed this way – similar to other current reduced-form biosphere models – does not take into account land-use change and the resulting loss of biological diversity and productivity. It also neglects a possible complete NPP saturation at a high CO_2 cut-off level as well as a possible accelerated respirative return of carbon to the atmosphere due to temperature and hydrological cycle feedbacks (cf. Joos et al., 2001).

In a manner similar to the procedure discussed above, the original impulse-response representation of the hypothetical terrestrial carbon sink arising from CO_2 fertilization of the land vegetation has been translated into a box-model describing the carbon fluxes between the atmosphere and four terrestrial carbon reservoirs. The respirational decay of the carbon additionally allocated in two of these carbon pools (boxes 1 and 2) is characterized by decay time constants shorter than the discretization time step of 5 years. These reservoirs can be assumed to be in instantaneous equilibrium with the atmosphere and treated as a single carbon pool containing $c_{Bc}(t)$ excess carbon.

As already indicated, typical TWA results such as emissions corridors or reachable climate domains are obtained by solving several independent dynamic optimization problems. In order to allow GAMS to solve these problems numerically, all differential equations must be appropriately translated into difference equations that are subsequently interpreted as equality constraints linking the otherwise independent time-discrete values of the state and control variables involved. As a result of this procedure, the dynamic optimization problems are transferred into high-dimensional static optimization problems that can be tackled by suitable nonlinear solvers like CONOPT, bundled as part of the GAMS modeling platform.

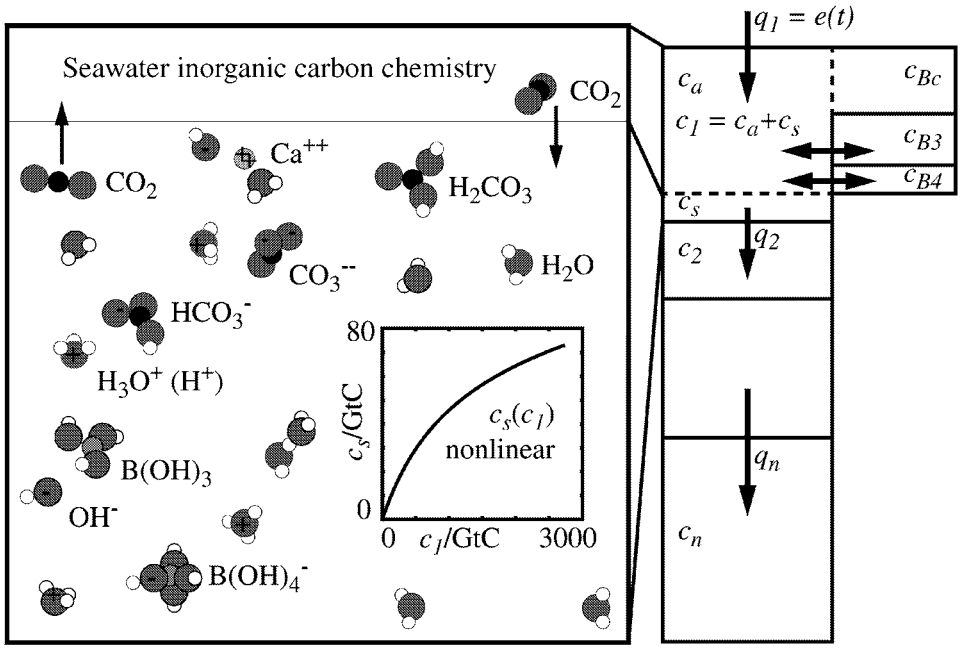

Figure 1. The ICLIPS carbon-cycle model. On the right, the cascade of oceanic layers, the uppermost of which represents the composite atmosphere-mixed layer, coupled to three terrestrial reservoirs. On the left, a zoom into the *composite* layer, for illustration of the nonlinear partitioning of the composite layer's carbon c_1 into its atmospheric and mixed-layer subsystems. c_a denotes the anthropogenic carbon in the atmosphere (in GtC), c_s the carbon perturbation in the oceanic mixed layer, and c_j the anthropogenic carbon in the jth oceanic layer. The model includes an explicit treatment of the nonlinear sea water inorganic carbon chemistry resulting in a decreasing solubility of additional CO_2 in sea water as the background concentrations rise. The resulting nonlinear relationship between anthropogenic carbon c_s in the oceanic mixed layer and anthropogenic carbon c_1 in the composite layer (comprising the oceanic-mixed layer and the atmosphere) is depicted explicitly. $e(t)$ denotes anthropogenic carbon emissions, q_j represents the carbon flux from layer $j-1$ into layer j, c_{Bi} is the anthropogenic carbon in land biosphere reservoir $i \in \{3, 4\}$, and c_{Bc} comprises the short term anthropogenic carbon in the biosphere (see also text).

The entire carbon chemistry as implemented in the NICCS model (Equations (44)–(63) in Hooss, 2001) can be reduced to a system of 5 coupled algebraic equations, which are treated as nonlinear equality constraints in the optimizing ICLIPS model. The complete carbon cycle dynamics can be described by 7 differential equations (Equation 90 in Hooss, 2001), which have been translated by using a predictor-corrector scheme into the corresponding difference equations of the ICLIPS model. Together these equations define a highly efficient description of the oceanic and terrestrial biosphere carbon cycle.

The carbon cycle module can be easily separated from the ICLIPS model and repackaged as a stand-alone GAMS model. When applied in the traditional *forward mode*, this module mimics a simulation model and calculates CO_2 concentration

time-series originating from predefined emission profiles. In this case, the input (emissions projections) uniquely determines the output (atmospheric concentrations). The optimization procedure therefore can stop immediately after the first feasible solution is found. When applied in an inverse mode, this model is capable of determining initially unknown parameters, like the CO_2 terrestrial vegetation fertilization factor, for instance, in order to achieve a balanced carbon budget in the reference period selected by the carbon cycle inter-model comparison study (IPCC, 1996).

2.2. MODELING NON-CO_2 GREENHOUSE GASES AND AEROSOLS

We adopted various components of MAGICC (Model for the Assessment of Greenhouse-gas Induced Climate Change; cf. Wigley, 1988; Wigley and Raper, 1992; Wigley, 1994; Osborn and Wigley, 1994; Wigley et al., 1996) in order to simulate the atmospheric chemistry of aerosols and major greenhouse gases other than CO_2 (CH_4, N_2O, halocarbons, SF_6, tropospheric and stratospheric O_3, and stratospheric water vapor) and to describe their radiative forcings (Shine et al., 1990). The atmospheric retention of N_2O, halocarbons, SF_6, and CH_4, for example, is modeled by applying a single well-mixed box model for each greenhouse gas. For N_2O, halocarbons, and SF_6, the removal rates are assumed to be proportional to the concentrations. In the case of CH_4, the removal rate depends on the concentration in a non-linear way. The components included are very similar or identical to the 'simple models' (Harvey et al., 1997) used by the IPCC for scenario analyses reported in the Second Assessment Report (IPCC, 1996). They combine a sufficiently accurate representation of the processes involved with high computational efficiency. Future versions of the ICLIPS model will include recently developed reduced-form models for aerosols and greenhouse gases other than CO_2 (cf. Joos et al., 2001; Ramaswamy et al., 2001; Myhre et al., 1998).

2.3. THE SCALED SCENARIO APPROACH AND EOF ANALYSIS

The basic functionality of the ICM components described so far is to translate emissions scenarios into temporal paths of greenhouse gas concentrations and associated radiative forcings. From these trajectories, global mean temperature anomalies as well as time-dependent spatially and seasonally explicit fields of changes in temperature, cloudiness, precipitation, humidity, and sea level can be derived, which feed into the climate impact modules (Füssel et al., 2003) of the ICLIPS model.

A common method for the efficient construction of regionally and seasonally explicit climate change projections is the so-called scaled scenario approach (Santer et al., 1990; Mitchell et al., 1999; Robock et al., 1993; Smith and Pitts, 1997). This approach describes future climate change by scaling spatial patterns of climate anomalies derived from general circulation model (GCM) forcing experiments by

the respective global mean temperature change. The scaled scenario approach assumes that changes in many climate variables depend linearly on changes in global mean temperature or can be approximated as such. While this method has already been used with the results of equilibrium GCM experiments, its validity could only be tested when results of long-term transient GCM integrations became available.

The best available method to separate the climate change signal from the noise present in a transient GCM forcing experiment and to assess the number of independent dimensions in the climate change signal is empirical orthogonal function (EOF) analysis (Peixoto and Oort, 1992; von Storch and Navarra, 1995). The first EOF can be associated with the dominating spatial pattern of anomalies which exists in a climate variable in terms of difference between the scenario and control runs together with its corresponding time-dependent amplitude. We applied the EOF analysis to the results of a long-term forcing experiment with the periodically-synchronously coupled GCM ECHAM3/LSG at T21 resolution (Voss et al., 1998; Voss and Mikolajewicz, 2001). In the scenario integration, the CO_2 concentration is increased four-fold from the present-day level over a period of 120 years and held constant for another 730 years. The deviations arising from using patterns other than those derived from ECHAM3/LSG are discussed in detail in Füssel et al. (2003).

Figure 2 shows some basic results of this EOF analysis. The upper diagram depicts the change in radiative forcing and associated time coefficients (principal components) for annually averaged changes in all pertinent climate variables. The EOF patterns of all climate variables have been rescaled such that the corresponding time coefficients reach identical values at the end of the 850-year simulation period. The temporal response to the (prescribed) change in radiative forcing differs clearly between sea-level rise and the atmospheric climate variables (such as temperature). Even though there is some variability also within the atmospheric group, the time coefficient for near-surface air temperature $PC^T(t)$ provides a good approximation of the time coefficients of the other atmospheric variables $PC^\alpha, \alpha \in \{P, CC, H\}$ (precipitation, cloud cover, humidity).

The fraction of the variance in a climate variable which cannot be explained by the first EOF is positively correlated to the degree of its natural year-to-year variability. This fact in itself should not be a surprise. The relevant question in this context is whether the higher EOFs do still represent a discernible climate change signal. Further examination of the model output does not support this interpretation. The time trajectories of the second EOF all fluctuate with apparent randomness around zero (Hooss et al., 2001). We thus conclude that the respective first EOF covers the overwhelming fraction of the simulated climate change signal for the annual averages of all pertinent climate variables.

The lower diagram of Figure 2 is based on separate EOF analyses for four seasons and depicts trajectories of the time coefficients for both annual and seasonal temperature change. The first EOF explains about 97% of the total variance in the regional climate anomalies for annually averaged temperature. For seasonal

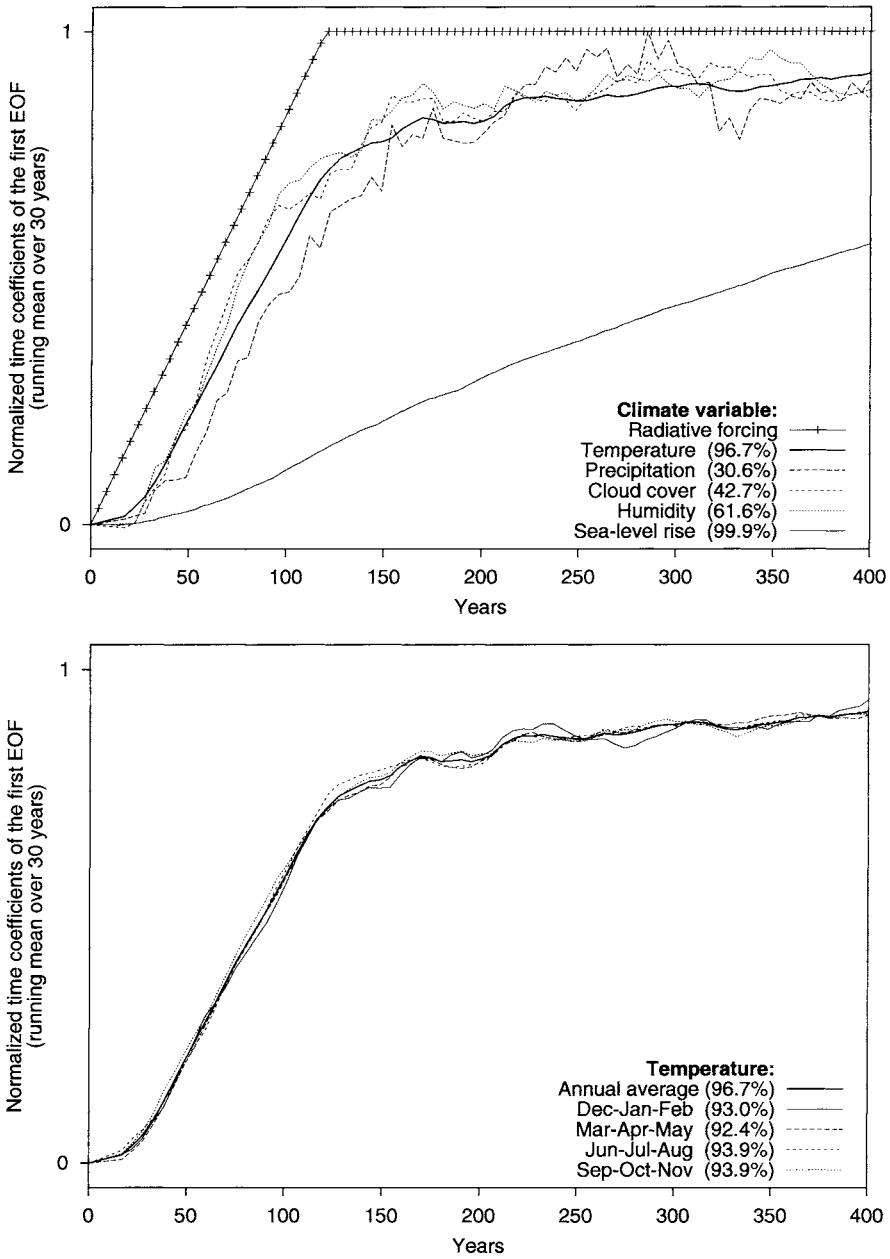

Figure 2. Trajectories of the normalized time coefficients (principal components or PC) of the first EOF (with a running mean over 30 years) for various climate variables during the first 400 years of the ECHAM3 experiment. The percentage of the variance in a climate variable that can be explained by the associated first EOF is given in brackets. *Top:* Radiative forcing and annual average temperature, precipitation, cloud cover, humidity, and sea-level rise. *Bottom:* Annual average temperature and seasonal temperature.

temperature change, between 92% and 94% of the simulated anomalies can be explained by the first seasonal EOF patterns. It is clear from the diagram that the time coefficient for annual temperature anomalies approximates well the time coefficients of the seasonal temperature anomalies. Similar results hold for the other climate variables.

The results of the EOF analysis depicted here allow us to conclude that the seasonal climate change signal simulated by ECHAM3 can be approximated by scaling appropriately normalized spatial patterns of the dominant seasonal climate anomalies for *each climate variable* (i.e., the respective first EOFs for temperature, precipitation, cloud cover, and humidity change) with the time-dependent magnitude of the change in *global mean temperature* (represented by the time coefficient PC^T of the first EOF for annual average temperature change). Due to the replacement of the PC trajectories of all seasonal atmospheric variables considered by just one (albeit differently normalized) time-dependent coefficient, namely the PC of annual mean temperature change, the number of differential equations to be solved in ICM in order to obtain scaling factors for the seasonal EOFs of the atmospheric variables is reduced by a factor of 16 (cf. Hooss, 2001). A fast reduced-form model is thus obtained. It is capable of providing information about seasonal and regional changes in near-surface air temperature, column-integrated cloud cover, precipitation, and humidity.

Framing the discussion in mathematical terms (cf. Joos et al., 2001), we obtain the following approximate description of the time-dependent regionally and seasonally explicit perturbation of a climate variable $V_s(t, \vec{x})$ (such as near-surface temperature T, cloud cover CC, precipitation P, humidity H) and the corresponding description of sea-level rise $SLR(t, \vec{x})$.

$$V_s(t, \vec{x}) \approx PC^T(t) \cdot EOF_s^V(\vec{x}) \tag{1}$$

$$SLR(t, \vec{x}) \approx PC^{SLR}(t) \cdot EOF^{SLR}(\vec{x}) \,, \tag{2}$$

where $PC^\alpha, \alpha \in \{T, SLR\}$, denote the first principal component of temperature change and sea-level rise. EOF_s^V and EOF^{SLR} are the dominant (for atmospheric variables season-dependent) spatial patterns (first EOF) of the signal. $\vec{x} = (x_1, x_2)$ is used to indicate longitude (x_1) and latitude (x_2). s distinguishes four different seasons. Note that here the EOF patterns are rescaled by a constant factor in order to compensate for the transition from PC^{CC}, PC^P, and PC^H to PC^T.

The time-dependent development of the first principal component PC^T (and the associated change in global mean temperature) can be approximated by an IRF (Hooss, 2001; Hooss et al., 2001; Prentice et al., 2001) driven by radiative forcing or, equivalently, by a corresponding differential equation model as implemented in the ICM. Following the approach of Joos et al. (2001) and thereby extending the original 'CO_2 only' case investigated by Hooss et al. (2001), radiative forcing entering this differential equation model is taken to be the sum of global mean radiative forcing from all greenhouse gases investigated and from aerosols. The

time evolution of $PC^{SLR}(t)$ is treated in a similar way (Hooss, 2001). It should be emphasized that the principal component $PC^{SLR}(t)$ and the associated EOF pattern correspond solely to sea-level rise originating from the thermal expansion of the ocean. The ICLIPS sea-level rise module is therefore supplemented by further components describing the sea-level rise resulting from the net melting of glaciers and small ice caps with contributions from Greenland and Antarctic ice sheets as given by Wigley and Raper (1993) and Warrick and Oerlemans (1990). The corresponding reduced-form models depend only on the evolution of global mean temperature, which means that they can be directly coupled with the differential equation model discussed above.

As already indicated, we used the Hamburg Model of the Ocean Carbon Cycle (HAMOCC) in order to determine the carbon cycle impulse response function. In contrast, the climate module converting radiative forcing into global mean temperature change and into spatial patterns of various climate variables is derived from the periodically-synchronously coupled ECHAM3/LSG general circulation model. It needs to be emphasized that achieving consistency between biogeochemical and energy balance components in an ideal fully integrated climate model would require that 'the same model be used to advect and diffuse heat as is used to advect and diffuse total dissolved carbon' (Harvey et al., 1997:30). Concerning the derivation of impulse response functions, this would imply using the same parent ocean model for both carbon cycle and climate modeling. In this respect, the ICM does not achieve full consistency, a weakness characterizing all reduced-form models used in the IPCC Second Assessment Report (IPCC, 1996; Harvey et al., 1997) and other prominent models like the Bern Carbon Cycle Model applied to derive the results of the IPCC Third Assessment Report (Prentice et al., 2001).

The numerical values of all parameters as well as calibrated initial values for all model variables are included in the self-documenting GAMS source code available from the authors. In order to facilitate uncertainty analysis, climate sensitivity is treated as an explicit parameter in ICM. Regional climate change patterns derived from the results of only one general circulation model still contain a considerable degree of uncertainty. Impact assessments based on *regionally differentiated* ICM output therefore should be accompanied by a sensitivity analysis that takes into account scaling patterns from different circulation models (cf. Füssel et al., 2003). The IRF method is, in principle, applicable to the climate change signal in any climate variable, including composite quantities and extreme value statistics if the signal is discernible in the GCM output and the samples are sufficiently large. Impulse response functions for calibration of the ICM modules can be extracted from the output of any transient climate-change GCM simulation. Thus, future ICM versions are planned to provide a variety of GCM IRF for selection.

3. Results

The ICM can be used in 'forward mode' for computing climate trajectories associated with exogenously defined greenhouse gas emissions scenarios. As part of the ICLIPS integrated assessment model, ICM is normally applied in 'inverse mode' and it provides dynamic restrictions for the computation of admissible emissions corridors (Toth et al., 2003a). Below we present the results of two applications that are obtained by using ICM in a stand-alone context, i.e., without coupling it to the economic and climate impact components of the full ICLIPS integrated framework.

3.1. COMPUTATION OF REACHABLE DOMAINS

Beyond being applied as part of the ICLIPS integrated assessment model to demarcate the emissions policy space under exogenously specified environmental and social targets, the novelty of ICM is its ability to establish *reachable climate domains* defined as feasible combinations of values of at least two model variables under given restrictions for plausible emissions scenarios. Extending the central methodological framework underlying the ICLIPS integrated assessment model (Bruckner et al., 2003), reachable domains can be determined for any combination of model variables by maximizing (minimizing) one variable while successively prescribing appropriate values for the others. This exercise draws heavily on the optimization capabilities of GAMS. An example of reachable climate domains (Figure 3) depicts all feasible combinations of the atmospheric CO_2 concentration and the globally averaged near-surface temperature for a given climate sensitivity of 2.5 °C under the following set of assumptions and restrictions defining the maximum plausible envelope for future greenhouse gas emissions.

- Two time horizons are considered: 2100 and 2200.
- As long as the remaining restrictions hold, energy-related CO_2, total anthropogenic CH_4 and N_2O emissions can be altered freely and independently.
- The rate of change for total anthropogenic CH_4 and N_2O emissions and for energy-related CO_2 emissions is restricted to $\pm 4\%$/year until 2100, and to $\pm 1\%$/year thereafter.
- Energy-related CO_2 emissions are bounded by the fossil fuel intensive SRES A1C-AIM scenario (IPCC, 2000) during the 21st century. After 2100, the upper bound increases by 1%/year.
- During the 21st century, the SRES A2 marker scenario – yielding the highest CH_4 and N_2O emissions out of all fully harmonized SRES scenarios (IPCC, 2000) – is used as an upper bound for total anthropogenic CH_4 and N_2O emissions. The upper bound remains constant thereafter.
- CO_2 emissions due to land-use change and SF_6 emissions are prescribed according to the SRES A2 marker scenario until 2100, and remain constant thereafter.

- Future halocarbon emissions are prescribed according to the Montreal Protocol and its amendments.
- SO_2 emissions are coupled to energy-related CO_2 emissions assuming a globally averaged desulfurization rate that may vary between 0.5% and 2%/year.

Although these assumptions are guided by the SRES scenarios (IPCC, 2000), they are obviously debatable. Their purpose here is to provide reasonable restrictions for the representative computation of reachable climate domains.

As Figure 3 clearly shows, a specific change in global mean temperature may come along with rather different CO_2 concentration levels and vice versa. The temperature spectrum associated with a given CO_2 concentration level can be explained by diverse preceding CO_2 emission paths or by different past or present concentration levels of the other greenhouse gases and aerosols. Furthermore, in the lower diagram of Figure 3, identical CO_2 concentration levels may be realized at different points in time. Contrary to popular perception, the related ambiguity can be tremendous even for a fixed climate sensitivity. Up until 2200, a CO_2 concentration level of 550 ppm, for example, may be accompanied by a change in global mean temperature between less than 1 °C or even more than 3 °C (with respect to the average climate through 1961–1990). Many ecosystems are sensitive to changes in climate as well as CO_2 concentration. An important lesson learnt from this exercise is that constraints on both drivers of ecosystem change are necessary if a specific impact level is not to be exceeded (Füssel et al., 2003).

Due to the lagged response of the climate system and to the additional CH_4 and N_2O accumulating between 2100 and 2200, the temperature range associated with a given CO_2 concentration level extends considerably towards higher temperature levels if 2200 instead of 2100 is used as the time horizon considered.

Figure 3 shows that the inertia of the CO_2-emitting economic system (operationalized by the restrictions for the emission scenarios) and the slow removal of carbon from the atmosphere lead to CO_2 concentrations above present-day levels throughout the 21st century. Although achievable in the 22nd century, CO_2 concentrations slightly below current levels would still be accompanied by considerably higher global mean temperatures due to the inertia of the climate system.

As indicated by the upper diagram in Figure 3, the lowest concentration values of the year 2100 and 2200 simultaneously define the lowest concentration values of the overall envelope depicted in the lower diagram for the time horizons 2100 and 2200, respectively. In other words, the lowest concentration levels reachable in the next 100 years (200 years) can only be realized in 2100 (2200) after the concentration profile associated with the emission profile that minimizes concentrations in 2100 (2200) has already culminated. As there is no additional scope for realizing lower concentrations, the respective emission profile is unique as are the emission profiles which maximize concentration levels in 2100 (2200). This explains the existence of horizontal parts of the envelopes depicted in Figure 3.

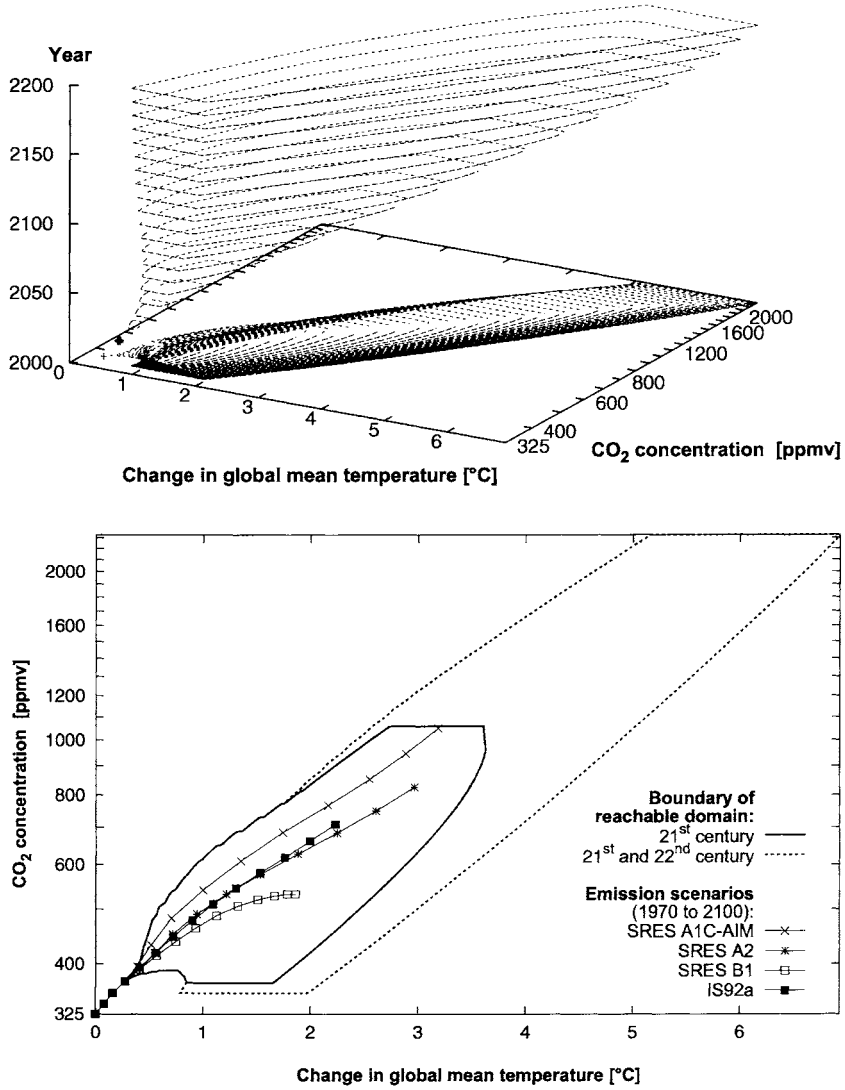

Figure 3. Top: Time evolution of the reachable climate domain. Depicted are the boundaries of the reachable domains for each point in time by dashed and dotted lines as well as their projections onto the temperature-concentration surface. The dashed (dotted) lines show the maximum (minimum) temperatures (specified with respect to the average climate of the period 1961–1990 for a climate sensitivity of 2.5 °C) compatible with the investigated CO_2 concentration levels for specific points in time. *Bottom:* Envelope of (the projections of) all time-dependent boundaries of the reachable climate domain until 2100 (solid lines) and 2200 (dashed lines). The results of a forward calculation for three SRES scenarios and one IS92 scenario are presented for comparison. The scenario trajectories depict the CO_2 concentration and the change in global mean temperature in decadal steps from 1970 until 2100. Further assumptions and the restrictions are discussed in the text.

The ambiguity of the temperature levels associated with the lowest and highest concentration levels originates from different radiative forcing contributions from CH_4, N_2O, and SO_2 emissions.

If an uncertainty interval for the climate sensitivity were used instead of a fixed value of 2.5 °C, the resulting reachable domains would become even wider. The approach presented here should not be confused with complementary efforts to display the climate-concentration combinations accessible via specific SRES scenarios (Figure 19-1 in Smith et al., 2001). This latter line of investigation delivers isolated results similar to the results for the different scenarios depicted in the lower diagram of Figure 3. The results discussed in Smith et al. therefore do not reveal those parts of the climate-concentration state space which are only accessible by purposeful but still constrained emissions mitigation policies.

3.2. SENSITIVITY ANALYSIS

The influence of various assumptions concerning CH_4 and N_2O on the shape of reachable climate domains is further investigated in a sensitivity analysis. The (wider) corridor labeled 'CH_4, N_2O flexible' in Figure 4 corresponds to the corridor for the 21st century in Figure 3. Another corridor is shown inside where CH_4 and N_2O concentrations are prescribed according to the SRES A2 scenario that previously defined the upper bound of their flexibility ranges. For a given CO_2 concentration level, maximum values for temperature change are therefore identical in both cases. Thus the related part of the reachable climate domain envelope is not altered. Prescribing high CH_4 and N_2O emissions, however, considerably increases the minimum temperatures associated with given CO_2 concentrations. Note that CH_4 and N_2O emissions in the SRES A1C-AIM scenario are lower than the prescribed ones. SRES A1C-AIM is therefore able to realize smaller minimum temperature changes for given CO_2 concentrations and consequently transgresses the boundary of the reachable domain in the prescribed emission case.

For low CO_2 concentration levels, the temperature ambiguity discussed above for variable, albeit constrained CH_4 and N_2O emissions diminishes for prescribed CH_4 and N_2O emissions. As a consequence, the horizontal line at the bottom of the reachable climate domain envelope does not exist in this case. The lower right corner of the reachable domain can be reached in 2100 by the most stringent CO_2 emission reductions permitted by the predefined constraints. The minimum temperature change in 2100 is about 0.85 °C for variable CH_4 and N_2O emissions, yet about twice that amount for prescribed (high) emissions. This result clearly emphasizes the importance of non-CO_2 emissions for long-term climate protection.

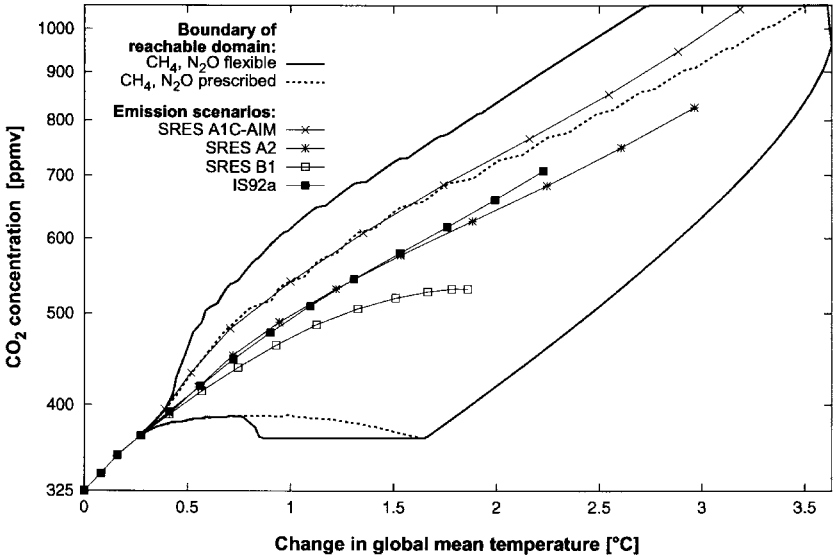

Figure 4. Boundaries of the reachable climate domains for variable and prescribed CH_4 and N_2O emissions depicted by bold lines and dotted lines, respectively. See Figure 3 for details concerning restrictions and assumptions.

4. Summary

The multi-forcing, multi-variable ICLIPS Climate Model (ICM) presented here is applied in the Potsdam model of Integrated assessments of CLImate Protection Strategies (ICLIPS). Linking the economic and the climate impact components in the ICLIPS framework, ICM takes into account all major greenhouse gases (CO_2, CH_4, N_2O, halocarbons, SF_6, tropospheric and stratospheric O_3, and stratospheric water vapor) as well as the radiative effects of aerosols originating from SO_2 emissions and from biomass burning. The output includes transient patterns of temperature, precipitation, humidity, and cloud cover change supplemented by transient information about various contributions leading to sea-level rise (thermal expansion of the ocean, melting of glaciers and ice sheets).

The carbon cycle module of ICM developed at the Max Planck Institute for Meteorology, Hamburg, consists of (a) a differential impulse-response representation of the 3-dimensional Hamburg Model of the Ocean Carbon Cycle (HAMOCC), extended into the nonlinear high-CO_2 domain by an explicit treatment of the chemistry governing CO_2 uptake through the ocean surface, and (b) a nonlinear differential impulse-response model of terrestrial biosphere CO_2 fertilization effects. Due to these enhancements, a carbon cycle model is obtained that mostly preserves the computational efficiency of the impulse-response approach while yielding plausible atmospheric concentrations for high-emission scenarios, i.e., beyond the linear regime. In order to be consistent with the results given in the

IPCC Second Assessment Report, we adopt parts of the MAGICC climate model to simulate the behavior of all non-CO_2 greenhouse gases as well as to describe their concentration-dependent radiative forcings. However, in order to avoid the related high computational burden, we do not apply the upwelling-diffusion model used by the IPCC for translating radiative forcing into global-mean temperature change. Instead, we include a highly efficient, nonlinearly forced differential impulse-response model of the principal component associated with the first EOF of changes in near-surface temperature. To further improve the computational efficiency, the spatial fields of changes in cloud cover, precipitation, and humidity are not driven by their own time-dependent amplitudes, but directly coupled to the evolution of near-surface temperature. The contribution of melting ice sheets and glaciers to sea level rise is computed with adapted versions of the models used for the IPCC Second Assessment Report.

In contrast to most contemporary intertemporal optimizing integrated assessment models (for a respective critique see: Joos and Bruno, 1996; Schultz and Kasting, 1997), the ICLIPS model includes carbon cycle and non-CO_2 chemistry as well as climate (in the strict sense) and sea-level rise modules which reflect a state-of-the-art understanding of the dynamic behavior of the systems involved.

Acknowledgements

The authors gratefully acknowledge helpful discussions with R. Voss, E. Maier-Reimer, F. Joos, and G. Petschel-Held as well as the financial support provided by the German Federal Ministry for Education, Science, Research and Technology (Contract No. 01 LK 9605/0).

References

Brooke, A., Kendrick, D., and Meeraus, A.: 1992, *GAMS, A User's Guide, Release 2.25*, The Scientific Press, San Francisco, CA.

Bruckner, T., Petschel-Held, G., Leimbach, M., and Toth, F. L.: 2003, 'Methodological Aspects of the Tolerable Windows Approach', *Clim. Change*, this issue.

Füssel, H.-M., Toth, F. L., van Minnen, J. G., and Kaspar, F.: 2003, 'Climate Impact Response Functions as Impact Tools in the Tolerable Windows Approach', *Clim. Change*, this issue.

Harvey, L. D. D.: 1989, 'Managing Atmospheric CO_2', *Clim. Change* **15**, 343–381.

Harvey, L. D. D., Gregory, J., Hoffert, M., Jain, A., Lal, M., Leemans, R., Raper, S. C. B., Wigley, T. M. L., and de Wolde, J. R.: 1997, 'An Introduction to Simple Climate Models Used in the IPCC Second Assessment Report', in Houghton, J. T., Meira Filho, L. G., Griggs, D. J., and Maskell, K. (eds.), *IPCC Technical Paper II*, IPCC, Geneva, Switzerland.

Hasselmann, K., Sausen, R., Maier-Reimer, E., and Voss, R.: 1993, 'On the Cold Start Problem in Transient Simulations with Coupled Atmosphere-ocean Models', *Clim. Dyn.* **9**, 53–61.

Hooss, K. G.: 2001, *Aggregate Models of Climate Change: Development and Applications*, Max Planck Institute for Meteorology, Examensarbeit 83, Dissertation am Fachbereich Geowissenschaften der Universität Hamburg, Hamburg, Germany.

Hooss, G., Voss, R., Hasselmann, K., Maier-Reimer, E., and Joos, F.: 2001, 'A Nonlinear Impulse Response Model of the Coupled Carbon Cycle – Climate System (NICCS)', *Clim. Dyn.* **18**, 189–202.

IPCC (Intergovernmental Panel on Climate Change): 1996, *Climate Change 1995: The Science of Climate Change*, Cambridge University Press, Cambridge, U.K.

IPCC (Intergovernmental Panel on Climate Change): 2000, *Special Report on Emissions Scenarios*, Cambridge University Press, Cambridge, U.K.

Joos, F. and Bruno, M.: 1996, 'Pulse Response Functions Are Cost-efficient Tools to Model the Link between Carbon Emissions, Atmospheric CO_2 and Global Warming', *Phys. Chem. Earth* **21**, 471–477.

Joos, F., Bruno, M., Fink, R., Siegenthaler, U., Stocker, T. F., LeQuéré, C., and Sarmiento, J.: 1996, 'An Efficient and Accurate Representation of Complex Oceanic and Biospheric Models of Anthropogenic Carbon Uptake', *Tellus* **48B**, 397–417.

Joos, F., Prentice, C., Sitch, S., Meyer, R., Hooss, G., Plattner, G.-K., Gerber, S., and Hasselmann, K.: 2001, 'Global Warming Feedbacks on Terrestrial Carbon Uptake under the Intergovernmental Panel on Climate Change (IPCC) Emission Scenarios', *Global Biogeochem. Cycles* **15**, 891–907.

Kicklighter, D. W., Bruno, M., Dönges, S., Esser, G., Heimann, M., Helfrich, J., Ift, F., Joos, F., Kaduk, J., Kohlmaier, G. H., McGuire, D., Melillo, J. M., Meyer, R., Moore, B., Nadler, A., Prentice, C., Sauf, W., Schloss, A. L., Sitch, S., Wittenberg, U., and Würth, G.: 1999, 'A First-order Analysis of the Potential Role of CO_2 Fertilization to Affect the Global Carbon Budget: A Comparison of Four Terrestrial Biosphere Models', *Tellus* **51B**, 343–366.

Leimbach, M. and Toth, F. L.: 2003, 'Economic Development and Emission Control over the Long Term: The ICLIPS Aggregated Economic Model', *Clim. Change*, this issue.

Maier-Reimer, E.: 1993, 'The Biological Pump in the Greenhouse', *Global Plan. Clim. Change* **8**, 13–15.

Maier-Reimer, E. and Hasselmann, K.: 1987, 'Transport and Storage of CO_2 in the Ocean – an Inorganic Ocean-circulation Carbon Cycle Model', *Clim. Dyn.* **2**, 63–90.

Meyer, R., Joos, F., Esser, G., Heimann, M., Hooss, G., Kohlmaier, G., Sauf, W., Voss, R., and Wittenberg, U.: 1999, 'The Substitution of High-resolution Terrestrial Biosphere Models and Carbon Sequestration in Response to Changing CO_2 and Climate', *Global Biogeochem. Cycles* **13**, 785–802.

Mitchell, J. F. B., Johns, T. C., Eagles, M., Ingram, W. J., and Davis, R. A.: 1999, 'Towards the Construction of Climate Change Scenarios', *Clim. Change* **41**, 547–581.

Myhre, G., Highwood, J., Shine, K. P., and Stordal, F.: 1998, 'New Estimates of Radiative Forcing Due to Well Mixed Greenhouse Gases', *Geophys. Res. Lett.* **25**, 2715–2718.

Osborn, T. J. and Wigley, T. M. L.: 1994, 'A Simple Model for Estimating Methane Concentrations and Lifetime Variations', *Clim. Dyn.* **9**, 181–193.

Peixoto, J. P. and Oort, A. H.: 1992, *Physics of Climate*, American Institute of Physics, New York, NY.

Petschel-Held, G. and Schellnhuber, H.-J.: 1997, 'The Tolerable Windows Approach to Climate Control: Optimization, Risks, and Perspectives', in Toth, F. L. (ed.), *Cost-benefit Analysis of Climate Change: The Broader Perspectives*, Birkhäuser, Basel, Switzerland, pp. 121–139.

Petschel-Held, G., Schellnhuber, H.-J., Bruckner, T., Toth, F. L., and Hasselmann, K.: 1999, 'The Tolerable Windows Approach: Theoretical and Methodological Foundations', *Clim. Change* **41**, 303–331.

Prentice, I. C. (co-ordinating lead author) et al.: 2001, 'The Carbon Cycle and Atmospheric Carbon Dioxide', in IPCC (Intergovernmental Panel on Climate Change), *Climate Change 2001: The Scientific Basis*, Cambridge University Press, Cambridge, U.K.

Ramaswamy, V. (co-ordinating lead author) et al.: 2001, 'Radiative Forcing of Climate Change', in IPCC (Intergovernmental Panel on Climate Change), *Climate Change 2001: The Scientific Basis*, Cambridge University Press, Cambridge, U.K.

Robock, A., Turco, R. P., Harwell, M. A., Ackerman, T. P., Andressen, R., Chang, H.-S., and Sivakumar, M. V. K.: 1993, 'Use of GCM Output for Impact Analysis', *Clim. Change* **23**, 293–335.

Santer, B. D., Wigley, T. M. L., Schlesinger, M. E., and Mitchell, J. F.: 1990, *Developing Climate Scenarios from Equilibrium GCM Results*, Report No. 47, Max Planck Institute for Meteorology, Hamburg, Germany.

Schultz, P. A. and Kasting, J. F.: 1997, 'Optimal Reductions in CO_2 Emissions', *Energy Policy* **25**, 491–500.

Shine, K. P., Derwent, R. G., Wuebbles, D. J., Morcrette, J.-J.: 1990, 'Radiative Forcing of Climate', in IPCC, *Climate Change: The IPCC Scientific Assessment*, Cambridge University Press, Cambridge, U.K., pp. 49–68.

Siegenthaler, U. and Joos, F.: 1992, 'Use of a Simple Model for Studying Oceanic Tracer Distributions and the Global Carbon Cycle', *Tellus* **44B**, 186–207.

Siegenthaler, U. and Oeschger, H.: 1978, 'Predicting Future Atmospheric Carbon Dioxide Levels', *Science* **199**, 388–395.

Siegenthaler, U. and Oeschger, H.: 1987, 'Biospheric CO_2 Emissions during the Past 200 Years Reconstructed by Deconvolution of Ice Core Data', *Tellus* **39B**, 104–154.

Smith, J. B. and Pitts, J. B.: 1997, 'Regional Climate Change Scenarios for Vulnerability and Adaptation Assessments', *Clim. Change* **36**, 3–21.

Smith, J. B., Schellnhuber, H.-J., Mirza, M. Q. (co-ordinating lead authors) et al.: 2001, 'Vulnerability to Climate Change and Reasons for Concern: A Synthesis', in IPCC (Intergovernmental Panel on Climate Change), *Climate Change 2001: Impacts, Adaptation, and Vulnerability*, Cambridge University Press, Cambridge, U.K., pp. 913–967.

Toth, F. L., Bruckner, T., Füssel, H.-M., Leimbach, M., and Petschel-Held, G.: 2003a, 'Integrated Assessment of Long-term Climate Policies: Part 2 – Model Results and Uncertainty Analysis', *Clim. Change*, this issue.

Toth, F. L., Bruckner, T., Füssel, H.-M., Leimbach, M., and Petschel-Held, G.: 2003b, 'Integrated Assessment of Long-term Climate Policies: Part 1 – Model Presentation', *Clim. Change*, this issue.

Toth, F. L., Bruckner, T., Füssel, H.-M., Leimbach, M., Petschel-Held, G., and Schellnhuber, H.-J.: 1997, 'The Tolerable Windows Approach to Integrated Assessments', in Cameron, O. K., Fukuwatari, K., and Morita, T. (eds.), *Climate Change and Integrated Assessment Models [IAMs] – Bridging the Gaps*, Proceedings of the IPCC Asia-Pacific Workshop on Integrated Assessment Models, Center for Global Environmental Research, Tsukuba, Japan, pp. 403–430.

von Storch, H. and Navarra, A. (eds.): 1995, *Analysis of Climate Variability: Applications of Statistical Techniques*, Springer, Berlin, Germany.

Voss, R. and Mikolajewicz, U.: 2001, 'Long-term Climate Changes Due to Increased CO_2 Concentration in the Coupled Atmosphere-ocean General Circulation Model ECHAM3/LSG', *Clim. Dyn.* **17**, 45–60.

Voss, R., Sausen, R., and Cubasch, U.: 1998, 'Periodically Synchronously Coupled Integrations with the Atmosphere-ocean General Circulation Model ECHAM3/LSG', *Clim. Dyn.* **14**, 249–266.

Warrick, R. A. and Oerlemans, J.: 1990, 'Sea Level Rise', in IPCC, *Climate Change: The IPCC Scientific Assessment*, Cambridge University Press, Cambridge, U.K., pp. 257–282.

WBGU (German Advisory Council on Global Change): 1995, *Scenario for the Derivation of Global CO_2 Reduction Targets and Implementation Strategies*, WBGU, Bremerhaven, Germany.

WBGU (German Advisory Council on Global Change): 1996, *World in Transition: Ways Towards Global Environmental Solutions*, Springer, Berlin, Germany.

Wigley, T. M. L.: 1994, *MAGICC (Model for the Assessment of Greenhouse-gas Induced Climate Change): User's Guide and Scientific Reference Manual*, National Centre for Atmospheric Research, Boulder, CO.

Wigley, T. M. L.: 1988, 'Future CFC Concentrations under the Montreal Protocol and their Greenhouse-effect Implications', *Nature* **335**, 333–335.

Wigley, T. M. L. and Raper, S. C. B.: 1992, 'Implications for Climate and Sea Level Rise of Revised IPCC Emission Scenarios', *Nature* **357**, 293–357.

Wigley, T. M. L. and Raper, S. C. B.: 1993, 'Future Changes in Global Mean Temperature and Sea Level', in Warrick, R. A., Barrow, E. M., and Wigley, T. M. L. (eds.), *Climate and Sea Level Change: Observations, Projections and Implications*, Cambridge University Press, Cambridge, U.K., pp. 111–133.

Wigley, T. M. L., Raper, S. C. B., and Salmon, M.: 1996, *Source Code of the MAGICC Model (as Used in MiniCam, Version 2.0)*, Climate Research Unit, University of East Anglia, Norwich, U.K.

(Received 31 May 2001; in revised form 23 August 2002)